ANALYTICAL DESCRIPTION OF THERMAL AND STRUCTURAL STRAINS IN MULTIPASS GMAW SURFACING AND REBUILDING.

WINCZEK Jerzy, GAWROŃSKA Elżbieta

Czestochowa University of Technology, Czestochowa, Poland, EU
winczek@gmail.com; elzbieta.gawronska@icis.pcz.pl

Abstract

The paper presents the models of temperature field, phase transformation kinetics, the calculation of thermal and structural strains in a steel element during multi-pass Gas Metal Arc Weld surfacing. The temperature field is described analytically assuming a bimodal volumetric model of heat source and a semi-infinite body model of the surfaced (rebuilt) workpiece. The electric arc is treated physically as one heat source. Part of the heat is transferred by the direct impact of the electric arc, while another part of the heat is transferred to the weld by the melted material of the electrode. The temperature increments caused by overlaying consecutive welding sequences and self-cooling of previously heated areas are considered in the description. Kinetics of phase transformations during heating is limited by temperature values at the beginning and at the end of austenitic transformation, while the progress of phase transformations during cooling is determined on the basis of TTT-welding diagram and Johnson-Mehl-Avrami and Kolomogorov law for diffusive transformations, and Koistinen-Marburger for martensitic transformation. Total strains result from strain history in subsequent cycles of heating and cooling (as the result of the passage of the welding head) and are equal to the sum of thermal and structural strains induced by phase transformations in these cycles.

Keywords: multipass welding, temperature field, phase transformation, strains, GMA.

1. INTRODUCTION

Modeling of thermomechanical states in the surfacing or rebuilding by welding requires the determination of temperature field, the calculation of the shares of structural elements when taking into account their changes that occur as result of phase transformations and the determination of temporary and residual stresses. In order to calculate the strains one has to know not only the temperature and structures determining mechanical properties of the material, but also thermal and structural strains.

In case of multi-pass surfacing, the application of subsequent welds causes previous welds to heat up and melt. During subsequent thermal cycles the material in a heat affected zone can undergo multiple phase transformations leading to the diversification of the structure between welds and in the heat affected zone also results in diversified thermal and structural strains.

2. THE MODEL OF TEMPERATURE FIELD

Many researchers have tried to obtain a solution, which would be closest to the real temperature distribution, using analytical methods as well as FEM. With reference to temperature field analysis during multi-pass welding, works concern mainly FEM [1 – 6]. In majority of existing solutions for temperature field only direct effects of electric arc heat on the material of welded or surfaced object are taken into account. Analyses of metallographic specimens of surfaced elements [7] indicate that fusion lines have more irregular shapes. In the description, the bimodal heat source model of the temperature field is presented. The electric arc was treated physically as one heat source, whose heat was divided: part of the heat is transferred by the direct

impact of the electric arc, but another part of the heat is transferred to the weld by the melted material of the electrode. This allows for the formulation of the temperature field in the form:

$$T(x,y,z,t)-T_0 = T_a(x,y,z,t)+T_w(x,y,z,t) \quad (1)$$

where $T_a(x,y,z,t)$ and $T_w(x,y,z,t)$ are temperature fields caused respectively by the heat of direct impact of an electric arc and by the heat of the weld reinforcement (consumed to melt the electrode). Analytical description of the temperature field caused by the direct impact of the electric arc with Gaussian heat distribution is shown in [8], whereas considering the heat stored in the liquid metal imposed on the surface is presented in [9]. In the temperature field modeling during multi-pass surfacing it is necessary to take into account temperature increments, caused by overlaying consecutive welding sequences and the self-cooling of areas previously heated and weld overlaps. The temperature field during the application of *k*-th weld is then described by the relationship:

$$T(x,y,z,t)-T_0 = \sum_{j=1}^{k-1}\Delta T_j^C + \Delta T_{k\ j}^H \quad (2)$$

where: ΔT_j^C denotes the increment of temperature caused by already applied (cooling) *j*-th weld, while ΔT_j^H the increment of temperature during application of *k*-th weld. Whereas temperature field after application of all welds is described by:

$$T(x,y,z,t)-T_0 = \sum_{j=1}^{k}\Delta T_j^C \quad (3$$

The algorithm for the temperature field calculation during the multipass surfacing by welding is presented in [10], whereas analytical description of the temperature field taking into account the heat of the weld is presented in [9].

3. KINETICS OF PHASE TRANSFORMATION IN SOLID STATE

Kinetics of diffusion transformation are described by Johnson-Mehl-Avrami's and Kolomogorov's (JMAK) rules [11]. The amount of austenite φ_A created during heating of the ferrite-pearlitic steel is therefore defined according to the formula:

$$\varphi_A(T) = \sum_j \varphi_j^0\left(1-exp\left(-b_j(T)t^{n_j(T)}\right)\right)+\varphi_A^0 \quad (4)$$

where φ_j^0 constitutes initial share of ferrite ($j \equiv F$), pearlite ($j \equiv P$) and bainite ($j \equiv B$), φ_A^0 denotes the amount of residual austenite remaining from the previous welding thermal cycle, while constants b_j and n_j are determined using conditions at the beginning and the end of transformation:

$$n_j = [ln(ln(0.99))]/ln(A_1/A_3) \quad (5)$$

$$b_j = 0.01 n_j / A_1 \quad (6)$$

In welding processes the volume fractions of particular phases during cooling depend on the temperature, cooling rate, and the share of austenite (in the zone of incomplete conversion $0 \le \varphi_A \le 1$). In quantitative perspective the progress of phase transformation during cooling is estimated by using additivity rule by

volumetric fraction φ_j of created phase what can be expressed analogically to Avrami's formula [12] by equation:

$$\varphi_j(T,t) = \varphi_A \varphi_j^{max} \left\{1 - exp\left[b_j(T) t^{n_j(T)}\right]\right\} + \varphi_j^0 \tag{7}$$

where φ_j^0 is volumetric participation of *j*-th structural component, which has not been converted during the austenitization, φ_j^{max} is the maximum volumetric fraction of phase *j* for the determined cooling rate estimated on the basis of the continuous cooling diagram (Fig. 2) while the integral volumetric fraction equals:

$$\sum_{j=1}^{k} \varphi_j = 1 \tag{8}$$

and *k* denotes the number of structural participations.

The quantitative description of the dependence of material's structure and quality of temperature and transformation time of over-cooled austenite during surfacing is made in accordance with the time-temperature-transformation diagram during continuous cooling, which binds the time of cooling $t_{8/5}$ (time when material stays within the range of temperature between 500 [^{0}C] and 800 [^{0}C], or the velocity of cooling ($v_{8/5}$ = (800-500)/$t_{8/5}$) and the temperature with the progress of phase transformation (Fig. 2). Those diagrams are called TTT–welding diagrams.

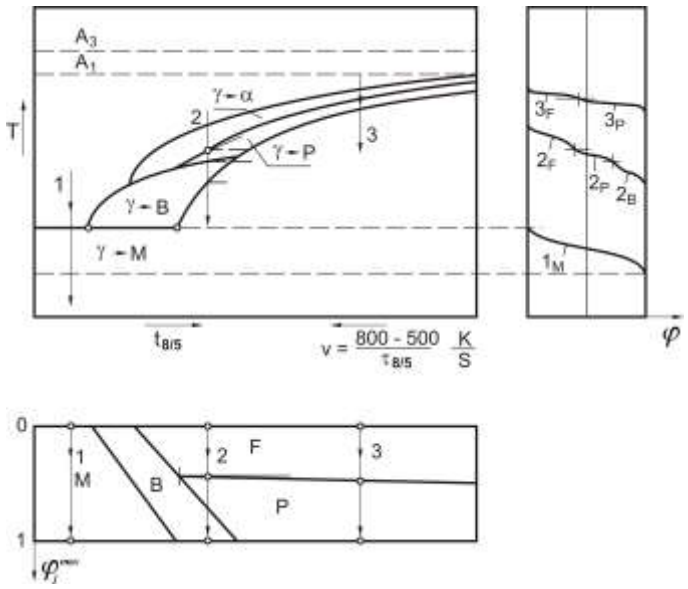

Fig. 2 Scheme of phase changes of overcooled austenite depending on cooling velocity within temperature range 800-500 ^{0}C

In quantitative perspective the progress of phase transformation is estimated by volumetric fraction φ_j of created phase, where *i* can denote ferrite (*j*≡*F*), pearlite (*j*≡*P*), bainite (*j*≡*B*) or martensite (*j*≡*M*). Volumetric fraction φ_j of created phase can be expressed using formula (7), in which time *t* is replaced with new independent variable – temperature *T* [13]:

$$\varphi_j = \varphi_A \varphi_j^{max} \left(1 - exp\left(-b_j(v_{8/5}) T^{n_j(v_{8/5})}\right)\right) + \varphi_j^0 \tag{9}$$

where

$$n_j = \left[ln\left(ln\left(1-\varphi_j^s\right)/ln\left(1-\varphi_j^f\right)\right)\right]/ln\left(T_j^s/T_j^f\right) \quad (10)$$

$$b_j = n_j\left(1-\varphi_j^f\right)/T_j^s \quad (11)$$

$T_j^s = T_j^s(v_{8/5})$ and $T_j^f = T_j^f(v_{8/5})$ are respectively initial and final temperature of the phase transformation of this component, φ_i^{max} denotes the maximal contribution of the phase i, which is then created from the cooled austenite.

The fraction of martensite formed below the temperature M_s is calculated using the Koistinen-Marburger formula [14,15]:

$$\varphi_M(T) = \varphi_A\varphi_M^{max}\left\{1-exp\left[-\mu(M_s-T)\right]\right\},\ \mu = ln\left(\varphi_M^{min}=0.1\right)/\left(M_s-M_f\right) \quad (12)$$

where φ_m denotes volumetric fraction of martensite, M_s and M_f denote initial and final temperature of martensite transformation respectively, T the current temperature of process.

4. THERMAL AND STRUCTURAL STRAINS

In the case of multiple reactions of the heat source the total distortion is the sum of thermical distortions and distortions caused by phasic changes in the following heating and cooling processes which result from the passage of electrode (a welding head) [10]. The total strain during single-pass surfacing represents the sum of thermal strains ε_j^H and ε_j^C caused by phase transformation during heating and cooling respectively:

$$\varepsilon(x,y,z,t) = \sum_{j=1}^{k}\varepsilon_j(x,y,z,t) \quad (13)$$

where:

$$\varepsilon_j(x,y,z,t) = \varepsilon_j^H + \varepsilon_j^C \quad (14)$$

ε_j^H and ε_j^C denote the thermal and structural strains during heating and cooling respectively while carrying the j-th bead.
Heating leads to the increase in the material's volume, while transformation of the initial structure (ferritic, pearlitic or bainitic) in austenite causes shrinkage connected to different density levels of given structures. Then strains during heating are equal to:

$$\varepsilon_j^H = \varepsilon_j^{Th} - \varepsilon_j^{Trh} \quad (15)$$

where ε_j^{Th} is a strain caused by thermal expansion of the material [10]:

$$\begin{aligned}\varepsilon_j^{Th} = \sum_{i=A,P,F,B,M}&\left(\alpha_i\varphi_{i0}\left(T-T_{0j}\right)H\left(T_{A_1}-T\right)+\alpha_i\varphi_i\left(T_{A1}-T_0\right)H\left(T-T_{A_1}\right)+\right.\\&\left.+\alpha_i\varphi_i\left(T-T_{A_1}\right)H\left(T_{A_3}-T\right)H\left(T-T_{A_1}\right)+\varphi_i\eta_i\left(T-T_{A_1}\right)H\left(T-T_{A_1}\right)H\left(T-T_{A_3}\right)\right)\end{aligned} \quad (16)$$

while ε^{Trh} is a phase transformation strain during heating:

$$\varepsilon_j^{Trh} = \sum_{i=P,F,B,M}\varphi_i\gamma_{iA} \quad (17)$$

where: γ_{iA} – structural strain of *i-th* structure in austenite, T_0 – initial temperature, α_i - linear thermal expansion coefficient of *i-th* structure, and H(x) is the Heaviside step function defined as follows:

$$H(x)=\begin{cases}1 & for\ x>0\\ 0{,}5 & for\ x=0\\ 0 & for\ x<0\end{cases} \tag{18}$$

Cooling of the material causes its shrinkage, while transformation of austenite in cooling structures in turn causes the increase of its volume. It leads to complicated changes of strains dependent not only on current temperature of material during cooling but also on the initial and the final temperature of transformation of austenite into ferrite, pearlite, bainite or martensite as well as on volumetric shares of given structural constituents (including austenite). The strain during cooling can be described by relation:

$$\varepsilon_j^H = \varepsilon_j^{Th} + \varepsilon_j^{Trh} \tag{19}$$

where ε^{Tc} is the strain caused by thermal shrinkage of material [10]:

$$\varepsilon_j^{Tc} = \alpha_A(T-T_{SOL})H(T-T_s)+\alpha_A(T_s-T_{SOL})H(T_s-T)+\sum_{i=A,P,F,B,M}\alpha_i\varphi_i(T-T_{si})H(T_{si}-T) \tag{20}$$

while ε_j^{Trc} is the structural strain caused by phase transformation during cooling:

$$\varepsilon_j^{Trc} = \sum_{i=P,F,B,M}\eta_i\gamma_{Ai} \tag{21}$$

where T_{SOL} denotes solidus temperature, T_s – the initial temperature of phase transformation, T_{si} - the initial temperature of austenite transformation in *i*-th structure, $T_s = max\ \{T_{sF}, T_{sP}, T_{sB}, T_{sM}\}$, γ_{Ai} – structural strain of austenite in *i*-th structure. In addition, due to the limit on solid state of material:

$$\varepsilon(x,y,z,t)=0 \quad for \quad T>T_{SOL} \tag{22}$$

CONCLUSION

The presented analytical approaches allow for the computation of the temperature field, the volumetric participation of the structural phases and thermal and structural strains in multipass GMAW surfacing or rebuilding steel or cast steel elements.

Consequent it allow for: the determination of HAZ (including full and partial transformation zones, fusion zone), welding thermal cycles, the change of volume phase participations of the structural components and the strains caused by the temperature field and the phase transformations, the size and the structural composition of the material in HAZ, the effect of the temperature field and the structural composition on the formation and development of strains during the deposition process at any point of GMAW surfaced object.

REFERENCES

[1] REED R C, BHADESHIA H K D H A simple model for multipass steel welds. Acta Metallurgica et Materialia, Vol. 42, 1994, pp. 3663-3678.

[2] MURUGAN S., KUMAR P.V., RAJ B., BOSE M.S.C., Temperature distribution during multipass welding of plates, International Journal of Pressure Vessels and Pipping, Vol. 75, 1998, pp. 891 – 905.

[3] LINDGREN L.E., HEDBLOM E. Modelling of addition of filler material in large deformation analysis of multipass welding, Communications in numerical methods in engineering, Vol. 17, 2001, pp. 647-657.

[4] DENG D, MURAKAWA H. Numerical simulation of temperature field and residual stress in multi-pass welds in stainless steel pipe and comparison with experimental measurements. Computational Materials Science, Vol. 37, 2006, pp. 269-277.

[5] JIANG W, YAHIAOUI K, HALL F R, Finite element predictions of temperature distributions in a multipass welded piping branch junction. Journal of Pressure Vessel Technology, Vol. 127, 2005, pp. 7–12.

[6] HEINZE C, SCHWENK C, RETHMEIER M. Numerical calculation of residual stress development of multi-pass gas metal arc welding under high restraint conditions. Materials Design, Vol. 35, 2012, pp. 201–209.

[7] KLIMPEL A., BALCER M., KLIMPEL A.S., RZEZNIKIEWICZ A. The effect of the method and parameters in the GMA surfacing with solid wires on the quality of pudding welds and the content of the base material in the overlay. Welding International, Vol. 20, 2006,pp. 845-850.

[8] WINCZEK J. Analytical solution to transient temperature field in a half-infinite body caused by moving volumetric heat source, International Journal of Heat and Mass Transfer, Vol. 53, 2010, pp. 5774-5781.

[9] WINCZEK J. New approach to modeling of temperature field in surfaced steel elements, International Journal of Heat and Mass Transfer, Vol. 54, 2011, pp. 4702-4709.

[10] WINCZEK J. Modelling of temperature field and phase transformations in weld rebuilding elements, Informatics in Materials Technology, Vol. 2, No 4, 2004, pp. 121 – 137.

[11] PIEKARSKA W., KUBIAK M., BOKOTA A. Numerical simulation of thermal phenomena and phase transformations in laser-arc hybrid welded joint, Archives of Metallurgy and Materials, Vol. 56, 2011, pp. 409-421.

[12] AVRAMI, M., Kinetics of phase change. I. General theory, The Journal of Chemical Physics, Vol. 7, 1939, pp. 1103-1112.

[13] WINCZEK J., A simplified method of predicting stresses in surfaced steel rods, Journal of Materials Processing Technology, Vol. 212, 2012, 1080 – 1088.

[14] KOISTINEN D.P., MARBURGER R.E., A general equation prescribing the extent of the austenite-martensite transformation in pure iron-carbon alloys and plain carbon steels, Acta Metallurgica, Vol. 7, 1959, pp. 59-60.

[15] DOMAŃSKI T., BOKOTA A., Numerical models of hardening phenomena of tools steel base on the TTT and CCT diagrams, Archives of Metallurgy and Materials, Vol. 56, 2011, pp. 325 – 344.